

# Numerical study of pressure drop for a new fibrous media model

Zhou Bin<sup>1</sup> Paolo Tronville<sup>2</sup> Richard Rivers<sup>3</sup> Zhang Xiaosong<sup>1</sup>

(<sup>1</sup> School of Energy and Environment, Southeast University, Nanjing 210096, China)

(<sup>2</sup> Department of Energetics, Politecnico di Torino, Torino 10129, Italy)

(<sup>3</sup> EQS Inc., Louisville, KY 40204, USA)

**Abstract:** An open-source computational fluid dynamics (CFD) code named OpenFOAM is used to validate the flow field characteristics (flow patterns and pressure drop) around a single cylinder. Results show that OpenFOAM is suitable for simulating the low Reynolds number flow and Shaw's analytical expression is one of the solutions to Stokes' paradox. Experiments are performed on fibrous media and OpenFOAM simulation is carried out using the Tronville-Rivers two-dimensional random fiber model in terms of the characteristics of pressure drop. It is shown that the Kuwabara model predicts the pressure drop of fibrous filter media more accurately than the Happel model, and the experimental pressure drop is between simulated pressure drops with both non-slip and full-slip boundaries on fiber surfaces.

**Key words:** fibrous media; diameter distribution; pressure drop; computational fluid dynamics simulation

Fibrous filters, which have been widely installed in air conditioning systems, are used for depth filtration. The performance of fibrous filters is greatly influenced by the feature of filter media. The two main characteristics of filter media are pressure drop and particle capture efficiency, which are dependent on the characteristics of filter media, the properties of the air flow, and the nature of the aerosol particles. Much attention has been paid to the research on the effects of aerosol characteristics and operating conditions, but little theoretical research has been made for media properties. Contrary to the previous theoretical models<sup>[1-4]</sup>, a new random fiber model was proposed based on the measurement of fiber diameters using scanning electron microscope (SEM) images<sup>[5-6]</sup>. This model with realistic descriptions of real structures of filters is useful for the optimum design of new media or selection from available existing media.

Since this model is made of randomly distributed 2-D cylinders, the flow field around a single cylinder is fundamental for the whole model. Therefore, the capability of an open-source CFD code named OpenFOAM<sup>[7]</sup> for simulating the flow field around a single fiber and the one in the whole model is investigated. A comparison of the pressure drop between the cell model and the experiments is performed.

## 1 Model Description

Unlike woven fabrics which are made of uniform fibers,

fibrous filter media are composed of polydisperse fibers. As shown in Fig. 1, the SEM images of a portion of filter medium samples with the size of  $120\ \mu\text{m} \times 80\ \mu\text{m}$  are taken. To obtain reasonable statistical validity in describing such a random-diameter filter medium, hundreds of fibers are measured. Experimental results reveal that the fiber diameter distribution with fibrous filter media fits the log-normal distribution well<sup>[6]</sup>. As pointed out by Vaughan and Brown<sup>[8]</sup>, solid fraction can be measured from the cross-section of the media when the cross-section is perpendicular to the fiber axis. A typical cross-section made by Steffens and Coury<sup>[9]</sup> is shown in Fig. 2. A program using C++ is written to generate a random fiber model as shown in Fig. 3<sup>[6]</sup>. By comparison of Figs. 1 to 3, it is reasonable to conclude that this random fiber model is a good representation of real media.

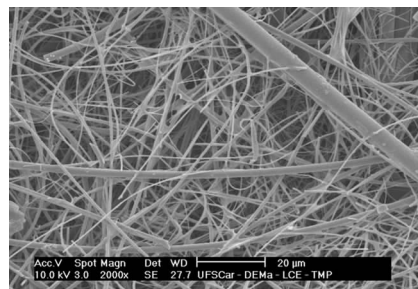


Fig. 1 SEM image of fibrous medium

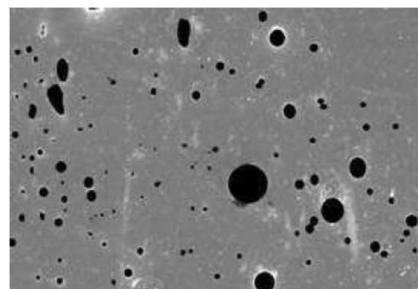


Fig. 2 Cross-section of fibrous medium

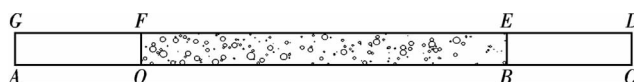


Fig. 3 Random fiber model

## 2 CFD Simulation of Single Cylinder

The random fiber model generated above is a 2-D model composed of log-normal distributed cylinders randomly positioned within the computational domain ( $O-B-E-F$ ). In order to obtain the flow field characteristics in this model, it is nec-

Received 2009-11-16.

**Biography:** Zhou Bin (1982—), male, doctor, zhoubinwx@hotmail.com.

**Foundation items:** China Scholarship Council Postgraduate Scholarship Program (No. 2007U20027), the National Natural Science Foundation of China (No. 50876020), the National Key Technology R&D Program of China during the 11th Five-Year Plan Period (No. 2008BAJ12B02).

**Citation:** Zhou Bin, Paolo Tronville, Richard Rivers, et al. Numerical study of pressure drop for a new fibrous filter media model[J]. Journal of Southeast University (English Edition), 2010, 26(2): 311–315.

essary to investigate the flow field around a single cylinder.

In air filtration applications, the fiber Reynolds number is extremely small (0.001 to 0.1)<sup>[10]</sup>, and, therefore, the low-Reynolds number flow is investigated here.

## 2.1 Single cylinder model

A benchmark test is performed on a single cylinder with the radius  $R = 1 \mu\text{m}$ , the characteristic length  $L = 100 \mu\text{m}$ , the air density  $1.2 \text{ kg/m}^3$  and the kinetic viscosity  $\nu = 15.17 \times 10^{-6} \text{ m}^2/\text{s}$ . The inlet velocity of the uniform flow is  $U = 0.0617 \text{ m/s}$ , so the Reynolds number is  $Re = 0.00813$ . The velocity fields are sampled according to Fig. 4. The existing utility named blockMesh in OpenFOAM is used to generate meshes. The generated structured mesh is presented in Fig. 5. OpenFOAM does not have constraints on the cell form, and it accepts unstructured meshes and all the kinds of polyhedral cells. Therefore, other mesh generators can be used as a preprocessor for an OpenFOAM simulation.

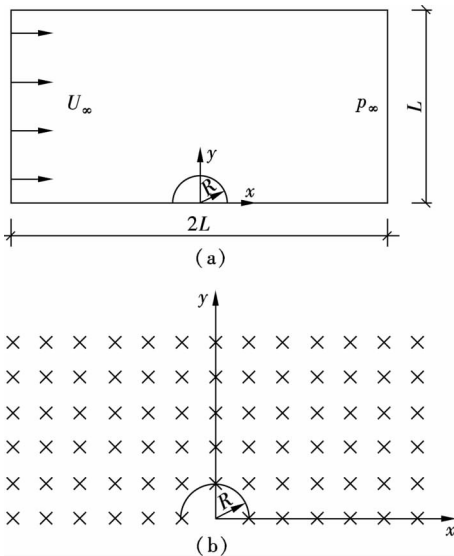


**Fig. 4** Single cylinder model and velocity sampling points. (a) Geometry of the flow around a cylinder; (b) Velocity sampling points around a cylinder

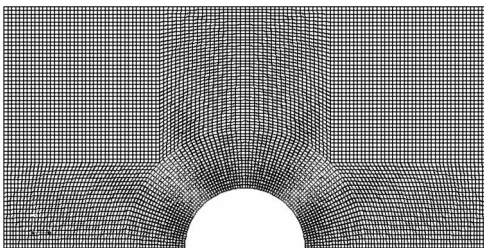


**Fig. 5** Mesh generated by blockMesh

## 2.2 Governing equation

Mass continuity and momentum equations for an incompressible flow are listed below:

$$\nabla \cdot \mathbf{U} = 0 \quad (1)$$

$$\text{div}(\rho \mathbf{U} \mathbf{U}) = -\nabla p + \text{div}(\mu \text{grad}(\mathbf{U})) \quad (2)$$

## 2.3 Boundary conditions

At the inlet, the constant uniform velocity is specified with  $U = (0.0617, 0, 0) \text{ m/s}$ . At the outlet, the constant pressure boundary condition is used ( $p = 0 \text{ Pa}$ ). On the isolated cylinder surface, the non-slip wall boundary is used. On the top and bottom walls, the symmetric boundary is used.

## 2.4 Initial conditions

The simulation generally starts from an initial solution and uses an iterative method, the SIMPLE algorithm, to reach a final flow field solution. Since it is a steady-state problem, the initial condition will not influence the simulation. The initial internal velocity and pressure fields are  $U = (0.0617, 0, 0) \text{ m/s}$  and  $p = 0 \text{ Pa}$ .

## 2.5 Results of single cylinder and discussion

It is well-known that there is a Stokes' paradox for the creeping flow around a cylinder, which means that there is no analytical solution when a non-slip boundary is implemented on the surface of the cylinder<sup>[11]</sup>. In order to validate the simulation results of OpenFOAM, a comparison between a potential flow field and different analytical solutions<sup>[12-19]</sup> is performed. A good agreement of dimensionless sampling velocities  $U_x^* = U_x/U_\infty$  between simulation and Shaw's solution is shown in Fig. 6.

Tab. 1 compares the values of drag coefficient  $C_D$  with the following definition:

$$C_D = \frac{F_D}{\frac{1}{2} \rho U^2 \times (2R)} \quad (3)$$

According to Tab. 1, results from Tomotika and Aoi<sup>[13]</sup>, Davies<sup>[14]</sup>, and Shaw<sup>[19]</sup> are quite similar for the Reynolds number between 0.001 and 0.1. White's expression<sup>[18]</sup> fits well with Tritton's experimental data<sup>[20]</sup>, but it is not valid when  $Re_f < 1$  where the drag coefficient is the smallest among these analytical solutions. The solution from Sucker and Brauer<sup>[17]</sup> is the biggest for the range of  $Re_f < 1$ , and attention should be paid that their expression is aimed to fit the experimental data from Ref. [20]. Actually, Kaplun<sup>[15]</sup> and Schlichting<sup>[16]</sup> derived the same expression.

**Tab. 1** Drag coefficients for low Reynolds number

$Re$	0.001	0.005	0.01	0.05	0.1
Ref. [13]	2 820.74	688.51	380.37	100.54	58.31
Ref. [15 - 16]	2 789.83	677.28	372.79	97.07	55.64
Ref. [14]	2 820.75	688.52	380.37	100.57	58.38
Ref. [17]	3 243.76	788.22	430.52	107.76	60.16
Ref. [18]	1 001.00	343.00	216.44	74.68	47.42
Ref. [19]	2 820.16	688.34	380.27	100.53	58.35

Since Davies' expression is validated by Finn's experiments at the Reynolds numbers from 0.06 to 0.5, it is clear that the expressions of Shaw, Tomotika and Aoi, and Davies can be used to validate CFD simulations, which is shown in Fig. 7.

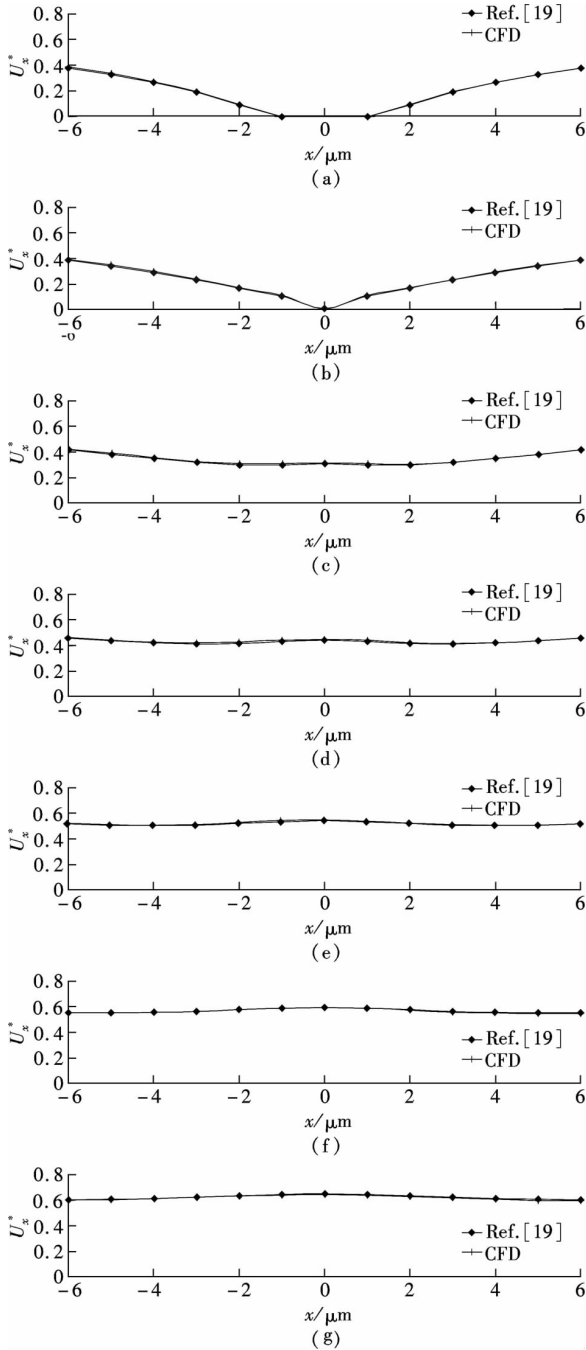


**Fig. 6** Comparison of velocity field between OpenFOAM and Shaw's solution with  $U_x^*$  value at the sampling line. (a)  $y = 0 \mu\text{m}$ ; (b)  $y = 1 \mu\text{m}$ ; (c)  $y = 2 \mu\text{m}$ ; (d)  $y = 3 \mu\text{m}$ ; (e)  $y = 4 \mu\text{m}$ ; (f)  $y = 5 \mu\text{m}$ ; (g)  $y = 6 \mu\text{m}$

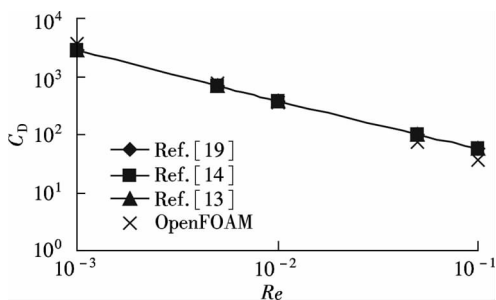


**Fig. 7** Comparison of drag coefficients between OpenFOAM and analytical solution

### 3 CFD Simulation and Experiment

The random fiber model is shown in Fig. 3. The governing equations are the same as those of the single cylinder case.

#### 3.1 Boundary conditions

The boundary conditions in the calculation domain are shown in Tab. 2, where the inlet velocity is set according to the experiment, and the outlet is set to be the pressure outlet.

**Tab. 2** Boundary conditions of random fiber models

Boundary	Conditions
<i>AG</i>	$U = U_0, \frac{\partial p}{\partial x} = 0$
<i>CD</i>	$\frac{\partial U}{\partial x} = 0, p = 0$
<i>A-O-B-C</i> and <i>G-F-E-D</i>	$U_x = U_y = 0, \frac{\partial p}{\partial y} = 0$
Fiber surfaces	Non-slip/slip boundary
<i>OF</i> and <i>BE</i>	Internal face

#### 3.2 Initial conditions

The initial internal velocity field is set as the experimental inlet velocity, and the pressure field  $p$  is set at 0 Pa.

#### 3.3 Results of random fiber model and discussion

According to Fig. 8 (a), the velocity distribution inside the filter media is quite complex, and the local velocity is small when several fibers are close to each other forming an “island”. The influence of the adjacent fiber on the flow field is great, and at different parts of the media, the effects are different. Therefore, theoretical models must consider the effects. From Fig. 8 (b), the pressure decreases gradually from the inlet to the outlet.

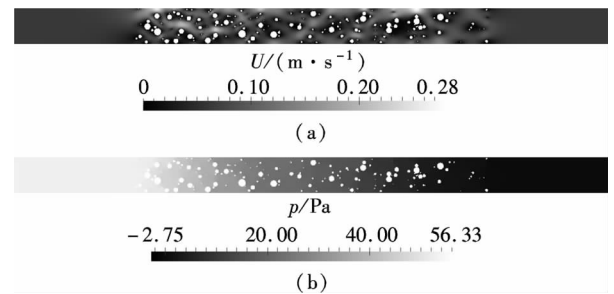


**Fig. 8** Simulated velocity field and pressure drop for random fiber model. (a) Velocity contour; (b) Pressure contour

### 4 Cell Models

Classical cell models proposed by Kuwabara<sup>[11]</sup> and Happel<sup>[2]</sup> consider inter-fiber effects. In Kuwabara's model, the inner cylinder is assumed to be stationary and the fluid goes through the unit cell. On the inner cylinder, there is no velocity, while on the outer envelope, there is no vorticity. In Happel's model, the inner cylinder moves at a constant velocity along the axis. As in Kuwabara's model, Happel implements the non-slip wall boundary condition on the inner cylinder, but no shear stress condition is used on the outer envelope. Kuwabara and Happel solved Stokes equations to

approximate the viscous flow through randomly distributed arrays of circular cylinders, respectively. Kuwabara and Happel obtained the following dimensionless pressure drop expressions, respectively:

$$\frac{\Delta p A R_f^2}{\mu Q h} = \frac{8\alpha}{-\ln\alpha + 2\alpha - \alpha^2/2 - 3/2} \quad (4)$$

$$\frac{\Delta p A R_f^2}{\mu Q h} = \frac{8\alpha}{-\ln\alpha - (1 - \alpha^2)/(1 + \alpha^2)} \quad (5)$$

## 5 Experiments

Experiments are performed by using an on-site air filter comparison tester (OSAFICT) in the Aerosol Technology and Filter Testing Laboratory, Politecnico di Torino, Italy. The air is drawn in by a centrifugal blower from the inlet. The tested filter is installed downstream of the prefilter. The pressure drop is measured with a manometer. The flow rate is measured with an orifice-plate flowmeter. After passing through the flowmeter, air turns around and arrives at the final filter installation position. The air is then exhausted with the blower. The schematic diagram of the test rig is shown in Fig. 9.

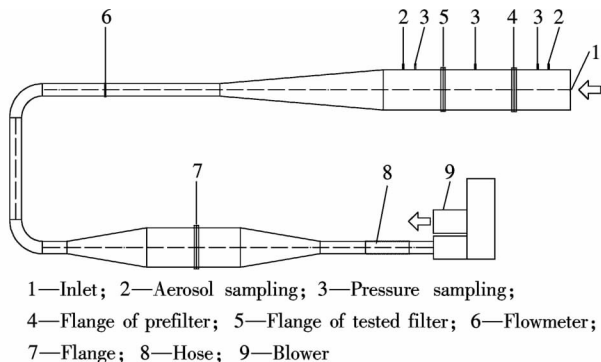


Fig. 9 Schematic diagram of the test rig

As shown in Fig. 10, the pressure drop characteristics of the medium fit well with Darcy's law, which means that the pressure drop is linearly proportional to the inlet velocity.

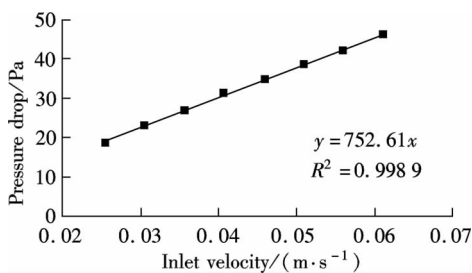


Fig. 10 Comparison between experimental pressure drop and fitted expression

## 6 Results and Discussion

Fig. 11 illustrates the pressure drop from OpenFOAM simulations, experiments and analytics. The Kuwabara model predicts the pressure drop more accurately than the Happel model, which is consistent with Yeh's findings<sup>[21]</sup>. The pres-

sure drop from Davies' expression is the smallest. The experimental pressure drop is between the simulated pressure drops with non-slip and full-slip boundaries on the cylinders, so partial slip boundaries should be studied in the future work.

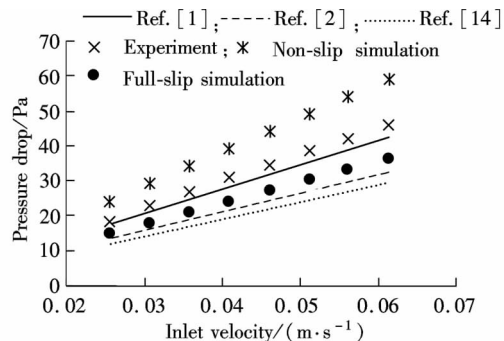


Fig. 11 Comparison of pressure drop among simulations, experiments and analytics

## 7 Conclusion

Shaw's analytical expression is found to be the solution to Stokes' paradox. OpenFOAM can simulate low Reynolds number flows ( $Re = 0.001$  to  $0.1$ ) in terms of velocity and drag coefficient. The inter-fiber effect is investigated with a random fiber model. The pressure drop from the Kuwabara model is found to be close to the experiment. The experimental pressure drop is between simulated pressure drops with both non-slip and full-slip boundaries.

## References

- [1] Kuwabara S. The forces experienced by randomly distributed parallel circular cylinders or spheres in a viscous flow at small Reynolds numbers [J]. *Journal of the Physical Society of Japan*, 1959, **14**(4): 527–532.
- [2] Happel J. Viscous flow relative to arrays of cylinders [J]. *American International Chemical Engineering Journal*, 1959, **5**(2): 474–477.
- [3] Kirsch A A, Stechkina I B. Air filtration [J]. *Journal of Aerosol Science*, 1995, **26**(S1): S61–S62.
- [4] Brown R C. Air filtration: an integrated approach to the theory and applications of fibrous filters [M]. Oxford: Pergamon Press, 1993: 40–50.
- [5] Tronville P, Rivers R D. Numerical modeling of the flow resistance of fibrous air filter media having random fiber diameter [C]//*Proceedings of Filtech 2005*. Wiesbaden, Germany, 2005: 261–268.
- [6] Zhou B, Tronville P, Rivers R. Generation of 2-dimensional models for CFD simulation of fibrous filter media with binder [J]. *Fibers and Polymers*, 2009, **10**(4): 526–538.
- [7] OpenCFD Ltd. OpenFOAM [EB/OL]. (2004-08-01) [2007-08-01]. <http://www.openfoam.com/>.
- [8] Vaughan N P, Brown R C. Observations of the microscopic structure of fibrous filters [J]. *Filtration & Separation*, 1996, **33**(8): 741–748.
- [9] Steffens J, Coury J R. Collection efficiency of fiber filters operating on the removal of nano-sized aerosol particles: II. Heterogeneous fibers [J]. *Separation and Purification Technology*, 2007, **58**(1): 106–112.
- [10] Fuchs N A. The mechanics of aerosols [M]. New York: Dover Publications, 1964: 203–216.

- [11] Stokes G G. On the effect of the internal friction of fluids on the motion of pendulums [J]. *Transactions of the Cambridge Philosophical Society*, 1851, **9**(2): 8 – 106.
- [12] Friedlander S K. Smoke, dust and haze, fundamentals of aerosol dynamics [M]. 2nd ed. Oxford: Oxford University Press, 2000.
- [13] Tomotika S, Aoi T. An expansion formula for the drag on a circular cylinder moving through a viscous fluid at small Reynolds numbers [J]. *The Quarterly Journal of Mechanics and Applied Mathematics*, 1951, **4**(4): 401 – 406.
- [14] Davies C N. Air filtration [M]. New York: Academic Press, 1973: 11 – 32.
- [15] Kaplun S. Low Reynolds numbers flow past a circular cylinder [J]. *Journal of Mathematics and Mechanics*, 1957, **6**(3): 595 – 603.
- [16] Schlichting H. Boundary-layer theory [M]. 6th ed. New York: McGraw-Hill Book Company, 1968.
- [17] Sucker D, Brauer H. Fluidodynamik bei der angestromten Zylindern [J]. *Warme und Stoffübertragung*, 1975, **8**(3): 149 – 158.
- [18] White F M. Viscous fluid flow [M]. 2nd ed. New York: McGraw-Hill, Inc, 1991.
- [19] Shaw W T. A simple resolution of Stokes' paradox?. arXiv: 0901.3621 [EB/OL]. (2009) [2009-10-10]. www.mth.kcl.ac.uk/~shaw/web\_page/papers/stokesnew.pdf.
- [20] Tritton D J. Experiments on the flow past a circular cylinder at low Reynolds numbers [J]. *Journal of Fluid Mechanics*, 1959, **6**(4): 547 – 567.
- [21] Yeh H C. A fundamental study of aerosol filtration by fibrous filters [D]. Minneapolis, MN, USA: University of Minnesota, 1972.

## 纤维滤料新模型的阻力数值模拟研究

周 斌<sup>1</sup> Paolo Tronville<sup>2</sup> Richard Rivers<sup>3</sup> 张小松<sup>1</sup>

(<sup>1</sup> 东南大学能源与环境学院, 南京 210096)

(<sup>2</sup> Department of Energetics, Politecnico di Torino, Torino 10129, Italy)

(<sup>3</sup> EQS Inc. , Louisville, KY 40204, USA)

**摘要:**利用流体力学开源代码 OpenFOAM 验证了单圆柱体周围的流体特性(包括流型和阻力),表明 OpenFOAM 能够用于模拟低  $Re$  数流,并发现 Shaw 的解析解是斯托克斯悖论的一种解.通过对纤维滤料进行试验以及对 Tronville-Rivers 二维纤维随机分布滤料新模型的阻力特性进行数值模拟,发现 Kuwabara 模型比 Happel 模型更能精确预测纤维滤料的阻力,而且试验阻力值介于纤维表面为无滑移和全滑移边界条件下的数值模拟值之间.

**关键词:**纤维滤料;直径分布;阻力;CFD 模拟

**中图分类号:** TU834.8